Chemical Science

ROYAL SOCIETY OF CHEMISTRY

EDGE ARTICLE

View Article Online
View Journal | View Issue





Cite this: *Chem. Sci.*, 2024, **15**, 2480

All publication charges for this article have been paid for by the Royal Society of Chemistry

Received 6th September 2023
Accepted 10th December 2023

DOI: 10.1039/d3sc04720b

rsc.li/chemical-science

# Mesoionic carbene-based self-assembled monolayers on gold†

Dianne S. Lee, [ab] Ishwar Singh, [ab] Alex J. Veinot, [bcd] Mark D. Aloisio, [ab] Justin T. Lomax, [bcd] Paul J. Ragogna [bc] and Cathleen M. Crudden [*ab]

N-Heterocyclic carbenes (NHC) have been widely studied as ligands for surface chemistry, and have shown advantages compared to existing ligands (*e.g.* thiols). Herein, we introduce mesoionic carbenes (MICs) as a new type of surface ligand. MICs exhibit higher σ-donor ability compared to typical NHCs, yet they have received little attention in the area of surface chemistry. The synthesis of MICs derived from imidazo[1,2-*a*]pyridine was established and fully characterized by spectroscopic methods. The self-assembly of these MICs on gold was analyzed by X-ray photoelectron spectroscopy (XPS). Additionally, XPS was used to compare bonding ability in MICs compared to the typical NHCs. These results show that MIC overlayers on gold are robust, resistant to replacement by NHCs, and may be superior to NHCs for applications that require even greater levels of robustness.

## Introduction

Since the first report of N-heterocyclic carbenes (NHCs) as ligands for gold surfaces by Siemeling and co-workers,[1] the use of these ligands on metallic[1–23] and non-metallic surfaces,[2,3] has attracted considerable attention, with Au substrates being most commonly employed.[1,4–23] NHC-based self-assembled monolayers (SAMs) have been integrated into molecular electronics,[24–26] and biosensors,[16,17,22,27] and employed in surface patterning,[13,28] illustrating the importance of this emerging class of ligands for planar metal surfaces. The stronger surface binding energies of NHCs compared to the other classic ligands, such as thiolates or phosphines[18,29] and their high potential for tunability[30–32] positions NHCs as ideal candidates for producing the next generation of nanomaterials.

Despite the high potential for structural and electronic variability with this class of ligand, most studies have focused on classical Arduengo-type NHCs,[18,19,33] with select exceptions of 1,2,4-triazolylidenes,[18] cyclic alkyl amino carbenes,[34,35] and cyclopropenylidenes.[36] Mesoionic carbenes (MICs)[37,38] are superior σ-donors compared to NHCs and are powerful ligands in organometallic chemistry. However, apart from the work of the Nazemi group highlighting the use of MICs on nanoparticles,[39,40] MICs are absent in the field of surface chemistry. Given the lack of experimental studies with this important class of carbene, and the possibility for enhanced properties of the resulting SAMs, we set out to explore these structural variants as ligands for self-assembled monolayers on gold.

To exclude steric issues, we focused on the imidazo[1,2-*a*]pyridine-type **MIC$^{iPr}$** as our target molecule, which is isostructural to the well-studied ligand **NHC$^{iPr}$** (Fig. 1b).[8,11,18] Tolman electronic parameter measurements indicate that MICs such as **MIC$^{iPr}$** are stronger σ-donors than many NHCs.[41] Crystallographic analyses of isostructural Pd complexes of NHCs and MICs, reveal identical steric environments at the Pd center.[42,43] Therefore, differences between the bonding of MICs and NHCs on gold should be isolated only to electronic effects. Synthetic routes to imidazo[1,2-α]pyridines with secondary aliphatic groups in the 3-position remain underdeveloped. Routes to branched 1,3-diaklylated imidazo[1,2-α]pyridinium

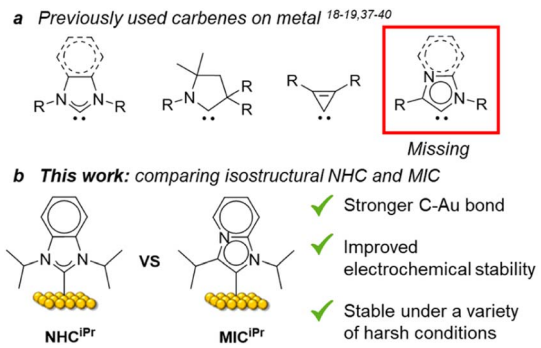


Fig. 1 (a) Previously used carbenes on metal surfaces, (b) molecular structures and the comparison between isostructural NHC and MIC self-assembled monolayers on Au surfaces.

[a]*Department of Chemistry, Queen's University, 90 Bader Lane, Kingston, Ontario, K7L 3N6, Canada. E-mail: cruddenc@chem.queensu.ca*

[b]*Carbon to Metal Coating Institute, C2MCI, Queen's University, 90 Bader Lane, Kingston, Ontario, K7L 4V1, Canada*

[c]*Department of Chemistry, Western University, London, Ontario N6A 3K7, Canada*

[d]*Surface Science Western, 999 Collip Cir, London, Ontario, N6G 0J3, Canada*

† Electronic supplementary information (ESI) available. See DOI: https://doi.org/10.1039/d3sc04720b

cations have not been reported in the literature. A sulfur-promoted oxidative cyclization reaction was recently disclosed using readily available aldehydes and 2-aminopyridine.[44] We examined this route, but the products of this reaction were invariably contaminated with sulfur impurities.[45] To prevent surface contamination by sulfur, an alternative synthetic route was developed (Scheme 1).

## Results and discussion

The desired MIC precursor **MIC$^{iPr}$·HI** was prepared using classical α-halocarbonyl chemistry.[46] Isovaleraldehyde was α-brominated using *N*-bromosuccinimide to afford **4** in 57% yield (Scheme 1). Reaction times longer than 2 h resulted in lower yields because of the reactive nature of α-halocarbonyl species, and thus **4** was used immediately without isolation. Reaction between an excess of **4** and 2-aminopyridine derivatives in refluxing ethanol afforded imidazo[1,2-*a*]pyridinium bromide salts **5·HBr** in up to 98% yield. Excesses of **4** were needed to prevent contamination with unreacted 2-aminopyridine. Analytically pure **5·HBr** could be isolated directly from the reaction mixture by first removing ethanol *in vacuo*, then suspending the resulting solids in diethyl ether and vacuum filtration. The route was amenable to the introduction of substituents on the backbone as needed (R = H, $CF_3$, OMe).

Alkylation of **5** with 2-iodopropane afforded **MIC$^{iPr}$·HI** in 82% yield. Reaction between **MIC$^{iPr}$·HI** and strong bases ($NaN(SiMe_3)_2$, $LiN(iPr)_2$, KH) resulted in decomposition, and attempts to trap the transient carbene with $CO_2$ to isolate a carboxylate derivative were unsuccessful. These difficulties led us to prepare the hydrogen carbonate salt **MIC$^{iPr}$·$H_2CO_3$**, which could be isolated in 78% yield as a monohydrate salt after resin exchange.[17] Imidazolium hydrogen carbonate salts are valuable air-stable precursors for generating NHC SAMs in solution and ultra-high vacuum (UHV).[5,6,13,17,25,27] Therefore, we expected that **MIC$^{iPr}$·$H_2CO_3$** would be similarly effective for producing MIC SAMs, however, initial attempts to prepare films by vapour phase deposition of **MIC$^{iPr}$·$H_2CO_3$** using techniques developed for **NHC$^{iPr}$** proved unsuccessful.

Thermogravimetric analysis (TGA) of **MIC$^{iPr}$·$H_2CO_3$** revealed that $CO_2$ and $H_2O$ are liberated around 160 °C, a higher temperature than **NHC$^{iPr}$·$H_2CO_3$**, which cleanly generates **NHC$^{iPr}$** between 100–120 °C.[47] This higher activation temperature is presumably required due to the higher p$K_a$ of the MIC precursor.[48] Beyond 160 °C, volatilization of **MIC$^{iPr}$·$H_2CO_3$** occurs, but is slower than **NHC$^{iPr}$·$H_2CO_3$** and has a temperature profile that suggests decomposition accompanies this process (Fig. S1†).

We next attempted to prepare SAMs of **MIC$^{iPr}$** on Au by immersing Au/Si samples in a 10 mM MeOH solution of **MIC$^{iPr}$·$H_2CO_3$** at room temperature for 24 h.[17] Although N 1s XPS analysis suggested that some deposition had occurred under these conditions (Fig. S10†), cyclic voltammetry (CV) and electrochemical impedance spectroscopy (EIS) showed no current suppression or increase in impedance, respectively (Fig. 2a and b), suggesting minimal deposition. However, increasing the deposition temperature to 50 °C and time to 48 h yielded SAMs with significant reduction in current and notable increase in resistance, as determined by CV and EIS, respectively, consistent with the formation of densely packed SAMs on the surface (Fig. 2a–c).

XPS analysis was employed to provide more insight into monolayer formation. We examined the XPS spectrum of the powdered **MIC$^{iPr}$·$H_2CO_3$** starting material (Fig. S8†), which was characterized by two signals in equal intensity assigned to the pyridyl and imine groups, at 401.6 eV and 400.6 eV respectively. XP spectra of SAMs resulting from deposition of **MIC$^{iPr}$·$H_2CO_3$** under optimized conditions also displayed two signals of equal intensity centered at 400.7 eV and 399.2 eV.[49] The shift in the binding energy and increase in the FWHM for both signals suggests a change in the electronics of the ligand upon binding to gold, and data strongly support the formation of an **MIC$^{iPr}$** SAM under these conditions.

SAMs of **MIC$^{iPr}$** were subjected to a variety of conditions including pH extremes (2, 12), refluxing water and 1% hydrogen peroxide for 24 hours. During these treatments, the **MIC$^{iPr}$** SAM showed minimal changes to the overall monolayer, as illustrated when comparing XPS signals in high resolution scans of C (1s), O (1s) and N (1s) (Fig. S11–S15†). To further probe the stability of these SAMs, we exposed **MIC$^{iPr}$** SAMs and **NHC$^{iPr}$** SAMs to pH 12 for five days. Analysis of the surface *via* time-of-flight secondary ion mass spectrometry (ToF-SIMS) showed

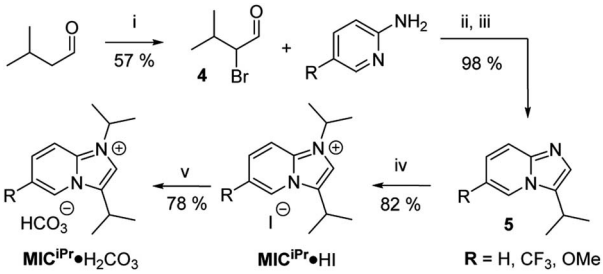


Scheme 1 Synthesis of **MIC$^{iPr}$·$H_2CO_3$**. (i) NBS, L-proline in DCM, 0 °C → RT; (ii) anhyd. EtOH Δ; (iii) aq. $NaHCO_3$; (iv) iPr-I, MeCN, Δ; (v) $HCO_3^-$ resin, MeOH, RT.

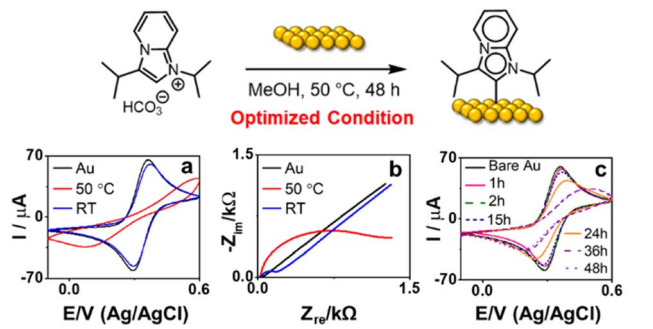


Fig. 2 Optimization of deposition conditions for **MIC$^{iPr}$·$H_2CO_3$** on Au using CV (a) and (b) EIS. Optimal conditions determined to be 10 mM **MIC$^{iPr}$·$H_2CO_3$** in MeOH at 50 °C for 48 h. (c) Optimization of time required for **MIC$^{iPr}$·$H_2CO_3$** deposition on gold by examination of CV curves.

virtually no loss of **MIC$^{iPr}$** on the surface even after exposure to these harsh conditions, while **NHC$^{iPr}$** was no longer observed (Fig. 3). This illustrates the improved robustness of SAMs designed from **MIC$^{iPr}$** under these extreme conditions.

To study the propensity for the two types of carbene to deposit on a bare gold surface, competition experiments were carried out at 50 °C for 48 hours with 10 mM **MIC$^{iPr}$·H$_2$CO$_3$** and 10 mM **CF$_3$·NHC$^{iPr}$·H$_2$CO$_3$** methanolic solution. To determine the surface coverage ratio between **MIC$^{iPr}$** and **CF$_3$·NHC$^{iPr}$**, the trifluoromethyl unit was employed as an XPS reporter along with N 1s signals (Fig. S18†). The average ratio between **MIC$^{iPr}$** and **CF$_3$·NHC$^{iPr}$** was calculated to be 4 : 1 (Table S1†), demonstrating the preferential formation of SAMs from **MIC$^{iPr}$** in comparison with **CF$_3$·NHC$^{iPr}$**. The inclusion of a CF$_3$ substituent had no effect on the binding strength of **CF$_3$·NHC$^{iPr}$** as shown by simple replacement tests between **NHC$^{iPr}$** and **CF$_3$·NHC$^{iPr}$** (Fig. S19†), since the final monolayer consists of both **NHC$^{iPr}$** and **CF$_3$·NHC$^{iPr}$** in a roughly 1 : 1 ratio. This ratio implies that the binding strengths of **NHC$^{iPr}$** and **CF$_3$·NHC$^{iPr}$** for SAM formation are comparable.

We then set out to compare the ability of one NHC to replace a preformed SAM of the other carbene. SAMs of **MIC$^{iPr}$** were prepared on Au/Si surfaces as previously described, and then treated with **CF$_3$·NHC$^{iPr}$·H$_2$CO$_3$** using the trifluoromethyl unit as an XPS reporter (Fig. 4). Typically, SAMs composed of benzannulated NHCs such as **NHC$^{iPr}$** are deposited over 24 h at room temperature, and so we employed these conditions to test the stability of **MIC$^{iPr}$** *vs.* replacement with **NHC$^{iPr}$**. After exposure to these conditions, no NHC was incorporated as determined by analysis of fluorine content in the F 1s region (Fig. 4 and Table 1, entry 1). This indicates that the **MIC$^{iPr}$** SAM resisted the incorporation of **CF$_3$·NHC$^{iPr}$** within the error of XPS measurements.

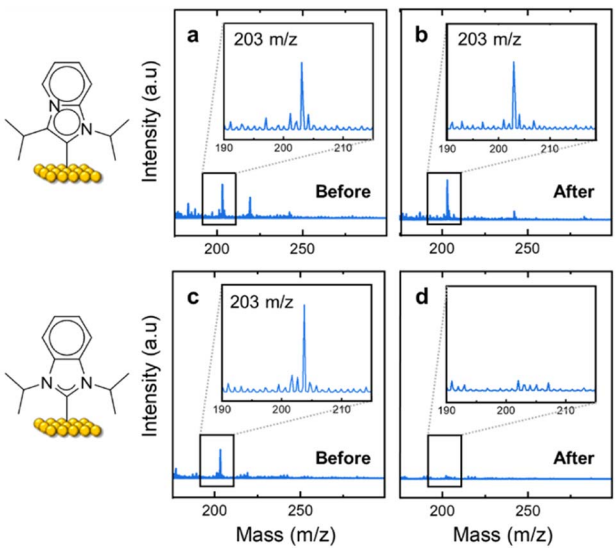


Fig. 3 ToF-SIMS data of MIC$^{iPr}$ and NHC$^{iPr}$ before and after stability test under pH 12 for 5 days. (a) MIC$^{iPr}$ before exposure; (b) MIC$^{iPr}$ after exposure; (c) NHC$^{iPr}$ before exposure; (d) NHC$^{iPr}$ after exposure.

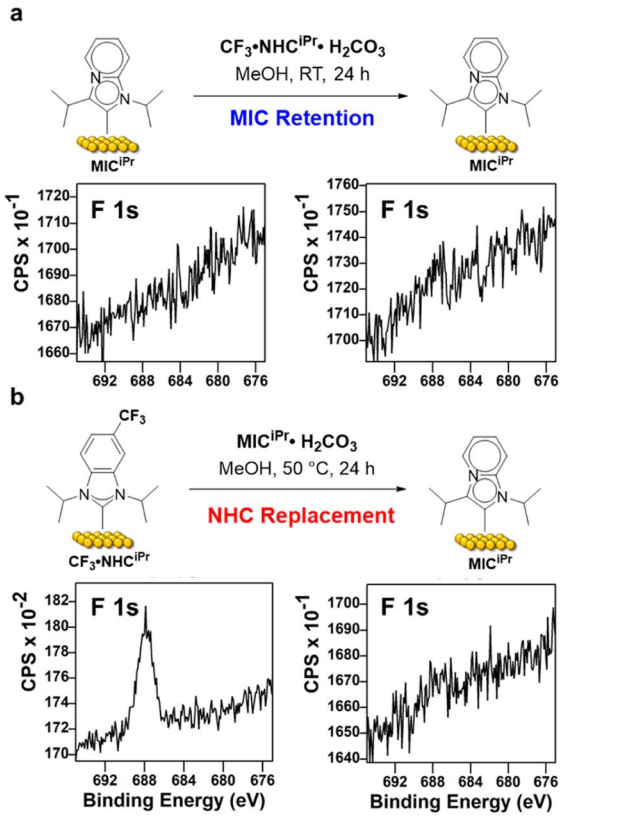


Fig. 4 F (1s) XPS regions of the replacement experiments between MIC$^{iPr}$ and CF$_3$·NHC$^{iPr}$ on Au surfaces. (a) MIC$^{iPr}$ replacement attempt with CF$_3$·NHC$^{iPr}$·H$_2$CO$_3$. (b) CF$_3$·NHC$^{iPr}$ replacement with MIC$^{iPr}$·H$_2$CO$_3$.

To test the reverse reaction, SAMs prepared from **CF$_3$·NHC$^{iPr}$** were treated with **MIC$^{iPr}$·H$_2$CO$_3$** and the loss or retention of fluorine was assessed by XPS (Fig. 4 and Table 1, entry 2). Under these conditions, we observed the complete removal of fluorine from the surface by XPS (Fig. 4 and Table 1, entry 2).

However, the need for elevated temperatures and longer deposition times to ensure generation of **MIC$^{iPr}$** from its bicarbonate salt is problematic for a direct comparison, and so an additional set of experiments were performed in which **MIC$^{iPr}$** SAMs were treated with **CF$_3$·NHC$^{iPr}$·H$_2$CO$_3$** at elevated temperatures and longer periods of time (Table 1, entries 3 and 4). Under these more forcing conditions, fluorine was observed by XPS analysis, but the replacement of **MIC** for **NHC** was minimal. Treatment of the **MIC$^{iPr}$** SAM with **CF$_3$·NHC$^{iPr}$·H$_2$CO$_3$** at RT for 48 h resulted in the incorporation of one **CF$_3$·NHC$^{iPr}$** for every six **MIC$^{iPr}$** units (Table 1; entries 3 and 4). At 50 °C for 48 h, one **CF$_3$·NHC$^{iPr}$** was incorporated for every five **MIC$^{iPr}$** units on Au. These results support the conclusion that MICs form more robust SAMs than those generated from typical NHCs, presumably due to stronger carbon–metal bonds on surfaces, consistent with the well-established molecular chemistry.[37,38]

Contact angle measurements were also performed for Au/Si substrates functionalized by **MIC$^{iPr}$** and **NHC$^{iPr}$** (Fig. S21 and

Table 1 Replacement experiments between $MIC^{iPr}$ and $CF_3{\cdot}NHC^{iPr}$ on Au surface

| Entry | Starting SAM | Replacement precursor | Temp. | Time | XPS (F : N) |
|---|---|---|---|---|---|
| 1 | $\mathbf{MIC^{iPr}}$ | $\mathbf{CF_3{\cdot}NHC^{iPr}{\cdot}H_2CO_3}$ | RT | 24 h | No fluorine |
| 2 | $\mathbf{CF_3{\cdot}NHC^{iPr}}$ | $\mathbf{MIC^{iPr}{\cdot}H_2CO_3}$ | 50 °C | 24 h | No fluorine |
| 3 | $\mathbf{MIC^{iPr}}$ | $\mathbf{CF_3{\cdot}NHC^{iPr}{\cdot}H_2CO_3}$ | RT | 48 h | 0.7 : 2 |
| 4 | $\mathbf{MIC^{iPr}}$ | $\mathbf{CF_3{\cdot}NHC^{iPr}{\cdot}H_2CO_3}$ | 50 °C | 48 h | 0.9 : 2 |

Table S2†). Compared to bare Au (67 ± 2°), the surface hydrophobicity does not change substantially upon the surface adsorption of $\mathbf{MIC^{iPr}}$ (72 ± 2°) and $\mathbf{NHC^{iPr}}$ (71 ± 2°).

## Conclusions

A straightforward synthetic route to the MIC precursor $\mathbf{MIC^{iPr}{\cdot}H_2CO_3}$ has been developed and its deposition on Au studied. Under optimized conditions, $\mathbf{MIC^{iPr}{\cdot}H_2CO_3}$ was deposited on Au surfaces, resulting in the formation of a new MIC-based SAM. Solution deposition conditions were optimized using electrochemical methods to monitor the successful formation of a stable monolayer. Monolayer stability was confirmed by multiple CV cycles and extreme potential range, concluding that solution deposition at 50 °C for 48 h was optimal.

The effect of the σ-donor ability of **MICs** *vs.* **NHCs** was demonstrated by a direct comparison of the two types of SAMs. This was accomplished through stability studies under extreme conditions, competitive deposition, and exchange studies by treatment of preformed monolayers with carbene precursors. These studies showed that MIC-based SAMs resist NHC incorporation, and NHC-based SAMs are replaced with MICs. When co-deposited, MICs out compete NHCs. Finally, MIC-based SAMs are more robust to long term (5 days) immersion in base. This study serves as the foundation for expanding the library of carbenes currently applied to surfaces for the next generation of carbene-based monolayers and providing more robust SAMs for use under harsher conditions. Future work in our lab will include finding appropriate conditions that allow for UHV studies of SAMs based on MICs, including spectroscopic and microscopic analyses.

## Experimental

### General methods

Unless otherwise stated, all solvents (including NMR solvents) and reagents were obtained from Sigma-Aldrich and used without further purification. Ethanol (anhydrous grade, Greenfield Global Commercial Alcohols) was stored over oven dried (150 °C) molecular sieves (3 Å, Alfa Aesar) prior to use. Using previously established methods,[1] hydrogen carbonate exchange resin was prepared by treating Amberlyst A26 hydroxide resin treated with carbon dioxide prior to use.

**Nuclear magnetic resonance (NMR) spectroscopy.** $^1$H, $^{13}$C $\{^1$H$\}$ and $^{19}$F$\{^1$H$\}$ NMR spectra were recorded at Queen's University using Bruker Avance-500, 600 or 700 MHz spectrometers at 298 K. Chemical shifts ($\delta$) are reported in parts per million (ppm) and are referenced to residual protonated ($^1$H) or deuterated ($^{13}$C$\{^1$H$\}$) solvent signals.[2] $^{19}$F$\{^1$H$\}$ NMR spectra are referenced to an external $CFCl_3$ standard ($\delta_F = 0$ ppm). Coupling constants ($J$) are reported as absolute values. All NMR data were processed and displayed using Bruker TopSpin software. Elemental analyses were performed at Queen's University using a Flash 2000 CHNS-O analyzer. Electrospray ionization mass spectra (ESI-MS) of small molecules were recorded at Queen's University using a Thermo Fisher Orbitrap VelosPro mass spectrometer with a heated-electrospray ionization probe.

**Electrochemical experiments.** All electrochemical experiments were carried out using a CHI6055E Electrochemical Analyzer potentiostat. All electrochemical experiments were performed using a three-electrode electrochemical cell set-up with 2 mm diameter gold disc working electrode. Ag/AgCl in 3 M KCl was used for a reference electrode, a platinum wire as counter/auxiliary electrode, and a salt bridge was used to allow free flow of ions between one cell to the other. The salt bridge was built using a 4 mm glass rod filled with a heated 2–5% agar solution in 1 M $KNO_3$ (w/v) and stored in 1 M $KNO_3$ solution. All electrochemical data were processed with OriginPro 2016 software.

**X-ray photoelectron spectroscopy (XPS).** XPS spectra were recorded on a Kratos Nova AXIS spectrometer equipped with AlN X-ray source. Samples were mounted on an aluminum sample holder using double-sided adhesive copper tape and kept under high vacuum ($10^{-8}$ Torr) overnight inside the preparation chamber before being transferred to the analysis chamber (ultra-high vacuum, $10^{-10}$ Torr). Data were collected using Al $K_\alpha$ radiation operating at 1486.69 eV (150 W, 15 kV), charge neutralizer and a delay-line detector (DLD) consisting of three multichannel plates. Acquired data were processed using CasaXPS software following reference handbooks. Processed data were plotted in Python using the Matplotlib package. Elemental compositions of samples were evaluated by running wide scan at 160 eV pass energy. After peak identification, high resolution scans were performed for O 1s, C 1s, N 1s, F 1s and substrate of interest region. These scans were performed at 20 eV pass energy. Au 4f spectra were peak fitted following guidelines from reference handbooks[3,4] and peak was charge corrected to 84 eV with spin–orbit coupling of ~3.7 eV. Unless otherwise specified, a Shirley type background correction was used for all spectra shown here.

**Time-of-flight secondary ion mass spectrometry (ToF-SIMS).** Samples were examined using an ION-TOF (GmbH) ToF-SIMS IV equipped with a Bi cluster liquid metal ion source. A pulsed 25 keV $Bi^{3+}$ cluster primary ion beam was used to bombard the surface of the samples to generate secondary ions

with a current of 1.5 μA. The positive (and negative) secondary ions were extracted from the sample surface, mass separated and detected *via* a reflectron-type of time-of-flight analyzer. Reflector values for the positive and negative mode were +16 V and −34 V, respectively. Sample charging was neutralized with a pulsed, low energy electron flood. Ion mass spectra were collected in an area of 500 μm × 500 μm at 128 × 128 pixels with 25 scans. Mass spectra were processed on ION-TOF software with a binning value of 256 and calibrated to H, C and $C_2H_5$ mass signals.

## Author contributions

This research was conceived and supervised by C. M. C. A. J. V. and I. S. performed the original synthesis and characterization of MICs. D. S. L. performed all of the electrochemical experiments. D. S. L. prepared XPS samples and analysed the samples with I. S. D. S. L. prepared ToF-SIMS samples and J. T. L. ran and analysed the samples. M. D. A. optimized and further characterized MICs. The manuscript was written and edited by D. S. L., A. J. V., I. S. and C. M. C.

## Conflicts of interest

There are no conflicts to declare.

## Acknowledgements

We would like to thank Queen's University, Canada Foundation for Innovation (CFI; CFI-33355), the Natural Sciences and Engineering Research Council of Canada (NSERC RGPIN/04667-2016; RGPIN/04377-2021), the New Frontiers in Research Fund – Transformation Program (NFRFT-2020-00573), and the Semiconductor Research Corporation are thanked for the financial support of this work. D. S. L. thanks Dr Gabriele Schatte for the assistance with XPS acquisition. A. J. V. thanks NSERC for the Vanier Scholarship and Banting Postdoctoral Fellowship. I. S. thanks the Ontario government for an Ontario Graduate Scholarship. J. T. L. thanks Drs Mark Biesinger and Heng-Yong Nie at Surface Science Western. C. M. C. thanks Queen's University, the Canada Foundation for Innovation, the Natural Sciences and Engineering Research Council of Canada (NSERC), and the New Frontiers in Research Fund – Transformation program.

## Notes and references

1 T. Weidner, J. E. Baio, A. Mundstock, C. Große, S. Karthäuser, C. Bruhn and U. Siemeling, *Aust. J. Chem.*, 2011, **64**, 1177–1179.
2 M. Franz, S. Chandola, M. Koy, R. Zielinski, H. Aldahhak, M. Das, M. Freitag, U. Gerstmann, D. Liebig, A. K. Hoffmann, M. Rosin, W. G. Schmidt, C. Hogan, F. Glorius, N. Esser and M. Dähne, *Nat. Chem.*, 2021, **13**, 828.
3 A. V. Zhukhovitskiy, M. G. Mavros, K. T. Queeney, T. Wu, T. Van Voorhis and J. A. Johnson, *J. Am. Chem. Soc.*, 2016, **138**, 8639–8652.
4 C. R. Larrea, C. J. Baddeley, M. R. Narouz, N. J. Mosey, J. H. Horton and C. M. Crudden, *ChemPhysChem*, 2017, **18**, 3536–3539.
5 S. Amirjalayer, A. Bakker, M. Freitag, F. Glorius and H. Fuchs, *Angew. Chem., Int. Ed.*, 2020, **59**, 21230–21235.
6 A. Bakker, A. Timmer, E. Kolodzeiski, M. Freitag, H. Y. Gao, H. Mönig, S. Amirjalayer, F. Glorius and H. Fuchs, *J. Am. Chem. Soc.*, 2018, **140**, 11889–11892.
7 G. Wang, A. Rühling, S. Amirjalayer, M. Knor, J. B. Ernst, C. Richter, H.-J. Gao, A. Timmer, H.-Y. Gao, N. L. Doltsinis, F. Glorius and H. Fuchs, *Nat. Chem.*, 2017, **9**, 152–156.
8 G. Lovat, E. A. Doud, D. Lu, G. Kladnik, M. S. Inkpen, M. L. Steigerwald, D. Cvetko, M. S. Hybertsen, A. Morgante, X. Roy and L. Venkataraman, *Chem. Sci.*, 2019, **10**, 930–935.
9 L. Jiang, B. Zhang, G. Médard, A. P. Seitsonen, F. Haag, F. Allegretti, J. Reichert, B. Kuster, J. V. Barth and A. C. Papageorgiou, *Chem. Sci.*, 2017, **8**, 8301–8308.
10 E. Angove, F. Grillo, H. A. Früchtl, A. J. Veinot, I. Singh, J. H. Horton, C. M. Crudden and C. J. Baddeley, *J. Phys. Chem. Lett.*, 2022, **13**, 2051–2056.
11 A. Inayeh, R. R. K. Groome, I. Singh, A. J. Veinot, F. C. de Lima, R. H. Miwa, C. M. Crudden and A. B. McLean, *Nat. Commun.*, 2021, **12**, 4034.
12 I. Singh, D. S. Lee, S. Huang, H. Bhattacharjee, W. Xu, J. F. McLeod, C. M. Crudden and Z. She, *Chem. Commun.*, 2021, **57**, 8421.
13 Z. She, M. R. Narouz, C. A. Smith, A. MacLean, H.-P. Loock, H.-B. Kraatz and C. M. Crudden, *Chem. Commun.*, 2020, **56**, 1275–1278.
14 A. J. Veinot, A. Al-Rashed, J. D. Padmos, I. Singh, D. S. Lee, M. R. Narouz, P. A. Lummis, C. J. Baddeley, C. M. Crudden and J. H. Horton, *Chem.–Eur. J.*, 2020, **26**, 11431–11434.
15 Z. Li, M. R. Narouz, K. Munro, B. Hao, C. M. Crudden, J. H. Horton and H. Hao, *ACS Appl. Mater. Interfaces*, 2017, **9**, 39223–39234.
16 Z. Li, K. Munro, I. I. Ebralize, M. R. Narouz, J. D. Padmos, H. Hao, C. M. Crudden and J. H. Horton, *Langmuir*, 2017, **33**, 13936–13944.
17 C. M. Crudden, J. H. Horton, M. R. Narouz, Z. Li, C. A. Smith, K. Munro, C. J. Baddeley, C. R. Larrea, B. Drevniok and B. Thanabalasingam, *Nat. Commun.*, 2016, **7**, 12654.
18 C. M. Crudden, J. H. Horton, I. I. Ebralidze, O. V. Zenkina, A. B. McLean, B. Drevniok, Z. She, H.-B. Kraatz, N. J. Mosey, T. Seki, E. C. Keske, J. D. Leake, A. Rousina-Webb and G. Wu, *Nat. Chem.*, 2014, **6**, 409.
19 A. V. Zhukhovitskiy, M. G. Mavros, T. Van Voorhis and J. A. Johnson, *J. Am. Chem. Soc.*, 2013, **135**, 7418–7421.
20 S. Dery, I. Berg, S. Kim, A. Cossaro, A. Verdini, L. Floreano, F. D. Toste and E. Gross, *Langmuir*, 2020, **36**, 697–703.
21 S. Dery, S. Kim, G. Tomaschun, D. Haddad, A. Cossaro, A. Verdini, L. Floreano, T. Klüner, F. D. Toste and E. Gross, *Chem.–Eur. J.*, 2019, **25**, 15067–15072.
22 J. F. DeJesus, M. J. Trujillo, J. P. Camden and D. M. Jenkins, *J. Am. Chem. Soc.*, 2018, **140**, 1247–1250.
23 M. J. Trujillo, S. L. Strausser, J. C. Becca, J. F. DeJesus, L. Jensen, D. M. Jenkins and J. P. Camden, *J. Phys. Chem. Lett.*, 2018, **9**, 6779–6785.

24 G. Foti and H. Vázquez, *Nanotechnology*, 2016, **27**, 125702.
25 G. Foti and H. Vázquez, *Beilstein J. Nanotechnol.*, 2017, **8**, 2060–2068.
26 E. A. Doud, M. S. Inkpen, G. Lovat, E. Montes, D. W. Paley, M. L. Steigerwald, H. c. Vázquez, L. Venkataraman and X. Roy, *J. Am. Chem. Soc.*, 2018, **140**, 8944–8949.
27 R. M. Mayall, C. A. Smith, A. S. Hyla, D. S. Lee, C. M. Crudden and V. I. Birss, *ACS Sens.*, 2020, **5**, 2747.
28 D. T. Nguyen, M. Freitag, M. Körsgen, S. Lamping, A. Rühling, A. H. Schaefer, M. H. Siekman, H. F. Arlinghaus, W. G. van der Wiel and F. Glorius, *Angew. Chem., Int. Ed.*, 2018, **57**, 11465–11469.
29 M. R. Narouz, K. M. Osten, P. J. Unsworth, R. W. Y. Man, K. Salorinne, S. Takano, R. Tomihara, S. Kaappa, S. Malola, C.-T. Dinh, J. D. Padmos, K. Ayoo, P. J. Garrett, M. Nambo, J. H. Horton, E. H. Sargent, H. Häkkinen, T. Tsukuda and C. M. Crudden, *Nat. Chem.*, 2019, **11**, 419–425.
30 C. A. Smith, M. R. Narouz, P. A. Lummis, I. Singh, A. Nazemi, C.-H. Li and C. M. Crudden, *Chem. Rev.*, 2019, **119**, 4986–5056.
31 M. N. Hopkinson, C. Richter, M. Schedler and F. Glorius, *Nature*, 2014, **510**, 485.
32 G. Kaur, R. L. Thimes, J. P. Camden and D. M. Jenkins, *Chem. Commun.*, 2022, **58**, 13188–13197.
33 L. M. Sherman, S. L. Strausser, R. K. Borsari, D. M. Jenkins and J. P. Camden, *Langmuir*, 2021, **37**, 5864–5871.
34 A. Bakker, M. Freitag, E. Kolodzeiski, P. Bellotti, A. Timmer, J. Ren, B. Schulze Lammers, D. Moock, H. W. Roesky, H. Mönig, S. Amirjalayer, H. Fuchs and F. Glorius, *Angew. Chem., Int. Ed.*, 2020, **59**, 13643–13646.
35 J. Ren, M. Freitag, Y. Gao, P. Bellotti, M. Das, B. Schulze Lammers, H. Mönig, Y. Zhang, C. G. Daniliuc, S. Du, H. Fuchs and F. Glorius, *Angew. Chem., Int. Ed.*, 2022, **61**, e202115104.
36 E. A. Doud, R. L. Starr, G. Kladnik, A. Voevodin, E. Montes, N. P. Arasu, Y. Zang, P. Zahl, A. Morgante and L. Venkataraman, *J. Am. Chem. Soc.*, 2020, **142**, 19902–19906.
37 Á. Vivancos, C. Segarra and M. Albrecht, *Chem. Rev.*, 2018, **118**, 9493–9586.
38 R. H. Crabtree, *Coord. Chem. Rev.*, 2013, **257**, 755–766.
39 D. T. H. Nguyen, M. Bélanger-Bouliga, L. R. Shultz, A. Maity, T. Jurca and A. Nazemi, *Chem. Mater.*, 2021, **33**, 9588–9600.
40 D. T. H. Nguyen, L. R. Shultz, T. Jurca and A. Nazemi, *Langmuir*, 2023, **39**, 3204–3215.
41 G. Song, Y. Zhang and X. Li, *Organometallics*, 2008, **27**, 1936–1943.
42 C.-H. Ke, B.-C. Kuo, D. Nandi and H. M. Lee, *Organometallics*, 2013, **32**, 4775–4784.
43 M. Heckenroth, A. Neels, M. G. Garnier, P. Aebi, A. W. Ehlers and M. Albrecht, *Chem.—Eur. J.*, 2009, **15**, 9375–9386.
44 J. Tan, P. Ni, H. Huang and G.-J. Deng, *Org. Biomol. Chem.*, 2018, **16**, 4227–4230.
45 Determined by elemental analysis (EA). EA was not reported in the published method.
46 R. Adams and J. S. Dix, *J. Am. Chem. Soc.*, 1958, **80**, 4618–4620.
47 M. Fèvre, P. Coupillaud, K. Miqueu, J.-M. Sotiropoulos, J. Vignolle and D. Taton, *J. Org. Chem.*, 2012, **77**, 10135–10144.
48 C. Barnett, M. L. Cole and J. B. Harper, *ACS Omega*, 2022, **7**, 34657–34664.
49 J. F. Moulder and J. Chastain, *Handbook of X-ray Photoelectron Spectroscopy: A Reference Book of Standard Spectra for Identification and Interpretation of XPS Data*, Physical Electronics Division, Perkin-Elmer Corporation, 1992.